Asian Journal of Chemistry; Vol. 29, No. 8 (2017), 1731-1734

ASIAN JOURNAL OF CHEMISTRY

https://doi.org/10.14233/ajchem.2017.20597

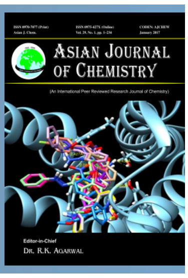

Electrochemical Characterization of Zn-Doped $LiNiMnCoO_2$ Cathode Materials for Li-Ion Battery

D. DEIVAMANI[*], P. PERUMAL, A.S. ENIGO CHITRA and M. BOOMASHRI

PG and Research Department of Physics, Alagappa Government Arts College, Karaikudi-630 003, India

*Corresponding author: E-mail: deivamaniaac@gmail.com

Received: 20 February 2017; *Accepted*: 11 April 2017; *Published online*: 12 June 2017; AJC-18432

This article mainly discusses on the performance of the layered Zn doped $LiNi_{0.3}Mn_{0.3}Co_{0.3}O_2$ positive electrode material for lithium ion battery. Zinc is substituted in place of Co to synthesize samples of Zn-doped Li $Ni_{0.3}Mn_{0.3}Co_{0.3-x}O_2$ (x = 0.00, 010, 0.02) cathode materials. Zinc substituted $LiNi_{0.3}Mn_{0.3}Co_{0.3-x}O_2$ positive active materials for lithium ion battery were synthesized by sol-gel procedure using metal acetates as starting material. The surface orientation, structure and electrochemical performance of calcined positive electrode materials were examined by scanning electron microscope, X-ray diffraction, electrochemical impedance spectroscopy and galvanostatic charge/discharge. The resistance components were derived from the impedance spectra and compared with discharge characteristics for a better performance. The cathode materials demonstrate a homogeneously distributed spherical morphology and exhibit a good reversibility. The Zn doped Li $Ni_{0.3}Mn_{0.3}Co_{0.29}Zn_{0.01}O_2$ cathode material synthesized at 1000 °C exhibits a high discharge capacity of 183.18 mAh/g at c/5 rate and offers better capacity retention of 85.47 % after formation cycles compared with the un-doped cathode material. The excellent cycle life performance can be attributed to the improvement in structure stability and lower resistance values which enhances the reaction kinetics.

Keywords: Cathode materials, Li-ion battery, Solution resistance, Charge transfer resistance.

INTRODUCTION

Many research works have been reported related to layered $LiNi_{0.3}Mn_{0.3}Co_{0.3}O_2$ [1,2] as it is capable of delivering high capacity and possesses safety features compared to $LiCoO_2$. Apart from the above qualities, this cathode material has a few restrictions, such as low rate performance arising from poor electronic conductivity and low capacity retention. These problems should be resolved before commercialization of this positive active material. One of the procedures is to improve the electrochemical performance by partially substituting oxides of manganese, cobalt and nickel, for transition metals such as iron, titanium, molybdenum or chromium and non-transition metals such as aluminum [3] or magnesium [4], which may standardize the layered structure with or without participating in the redox processes. This procedure also prevents any unwanted reactions between cathode and electrolyte. Up to now only a few researchers studied the electrochemical performance of the Zn-doped metal oxides [5]. This research work presents the performance study of Zn substituted $LiNi_{0.3}Mn_{0.3}Co_{0.3-x}Zn_xO_2$ materials prepared by sol-gel method [6]. Suresh *et al.* [7] have reported an improved capacity retention for layered $LiMn_{1-x}M_xO_2$ by Zn and Fe substitution. Deng *et al.* [8] carried out EIS studies to observe an improved diffusivity of Li ions by Zn substitution in $Li_2Fe_{0.97}M_{0.03}SiO_4$ cathode materials. The resistance values derived from the impedance spectrum explains the stability of the Zn substituted $LiNi_{0.3}Mn_{0.3}Co_{0.3}O_2$ positive active material for a better performance. The structural analysis and electrochemical performance of the layered $LiNi_{0.3}Mn_{0.3}Co_{0.3-x}Zn_xO_2$ materials were studied in this paper. The very low quantity of Zn substitution enhances the discharge capacity of $LiNi_{0.3}Mn_{0.3}Co_{0.3}O_2$ cathode material.

EXPERIMENTAL

Stoichiometric amounts of lithium acetate $[Li(CH_3COO)\cdot 2H_2O]$, nickel acetate $[Ni(CH_3COO)_2\cdot 4H_2O]$, manganese acetate $[Mn(CH_3COO)_2\cdot 4H_2O]$ and cobalt acetate $[Co(CH_3COO)_2\cdot 4H_2O]$ were mixed thoroughly and dissolved in de-ionized water. This solution was stirred constantly till it reaches homogeneity. Citric acid was made up to 150 mL with mild heating till it reaches complete homogeneity and this solution was added into the above metal acetates solution to form a complex [9]. This complex facilitates one to one particle interaction in the formation of $LiNi_{0.3}Mn_{0.3}Co_{0.3-x}Zn_xO_2$ (x = 0, 0.01 and 0.02). Then the solution was stirred continuously with heating (70-80 °C) during which pH was measured. Here, ammonia was added to maintain the pH level between 8 and

9. A foamy gel was obtained. Simultaneously, the gel was dried overnight in an oven at 120 °C for 12 h to remove moisture and to obtain a dried mass. It was decomposed at 400 °C for 5 h in furnace and finally calcined at 800 and 1000 °C for 10 h.

Powder XRD patterns of bare $LiNi_{0.3}Mn_{0.3}Co_{0.3}O_2$ and Zn substituted $LiNi_{0.3}Mn_{0.3}Co_{0.3}O_2$ samples are shown in Fig. 1. X-ray phase analysis was performed using Philips X'Pert powder diffractometer with monochromatic CuK_α radiation. The scan range was $10° \leq 2\theta \leq 90°$ with a step increment of 0.02°.

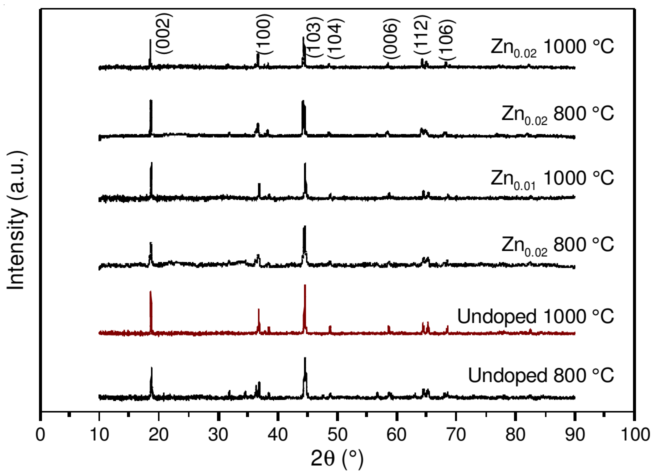

Fig 1. Diffraction patterns of bare $LiNi_{0.3}Mn_{0.3}Co_{0.3}O_2$ and Zn doped $LiNi_{0.3}Mn_{0.3}Co_{0.3}O_2$

Cathodes were prepared by coating viscous slurry on to Al foil consists of bare and Zn-doped cathode material. The cathode slurry was prepared using 80 % $LiNi_{05}Mn_{0.5}O_2$ synthesized sample, 15 % SP-carbon, 5 % PVdF (polyvinylidene fluoride) binder and few drops of NMP (N-methylpyrrolidone). 1 M $LiPF_6$ (lithium hexaflouro phosphate) was used as electrolyte dissolved in 1:1 / EC and DMC. Half cells (coin cells) were assembled in glove box filled with argon gas and O_2 and H_2O level is maintained at less than 0.1 ppm. Life cycle tests for the coin cells were performed using Arbin multichannel charge/discharge cycler up to 30 cycles between 4.2 and 2.8 V at 0.2C rate.

RESULTS AND DISCUSSION

X-ray diffraction: The XRD pattern of as prepared sample shows presence of major phase with less intensity due to amorphous state. Sol-gel experiments revealed that the crystallization process started at 800 °C and needs completion at higher temperatures to form pure phase with subsequent crystallinity. The sol-gel synthesized sample heated at 1000 °C exhibited X-ray diffraction pattern indicating sharp (b, d and f) and high intensity peaks due to crystallinity [10]. X-ray diffraction pattern of the sample heated at 1000 °C for 10 h indicates intensity of the (002) plane higher than (103) plane. Splitting of the (006)/(100) plane and (112)/(106) plane indicates the formation of cation ordered phase and high crystallinity.

Morphology and compositional analysis: The scanning electron micrographs of the bare and Zn substituted $LiNi_{0.3}Mn_{0.3}Co_{0.3}O_2$ cathode materials are shown in Fig. 2. The SEM images showed particles having good crystalline structure [11]. The images indicate uniform spherical morphology and particle size ranges from 200 and 250 nm for calcinations at 800 and 1000 °C, respectively. Particle size of the Zn substituted $LiNi_{0.3}Mn_{0.3}Co_{0.3}O_2$ (x = 0.02) cathodes at 800 °C is less than the Zn substituted $LiNi_{0.3}Mn_{0.3}Co_{0.3}O_2$ (x = 0.02) cathodes at 1000 °C uniform particle distribution and regular morphology also observed from the SEM image. Each of the spherical particles was built of large number of fine crystalline particles.

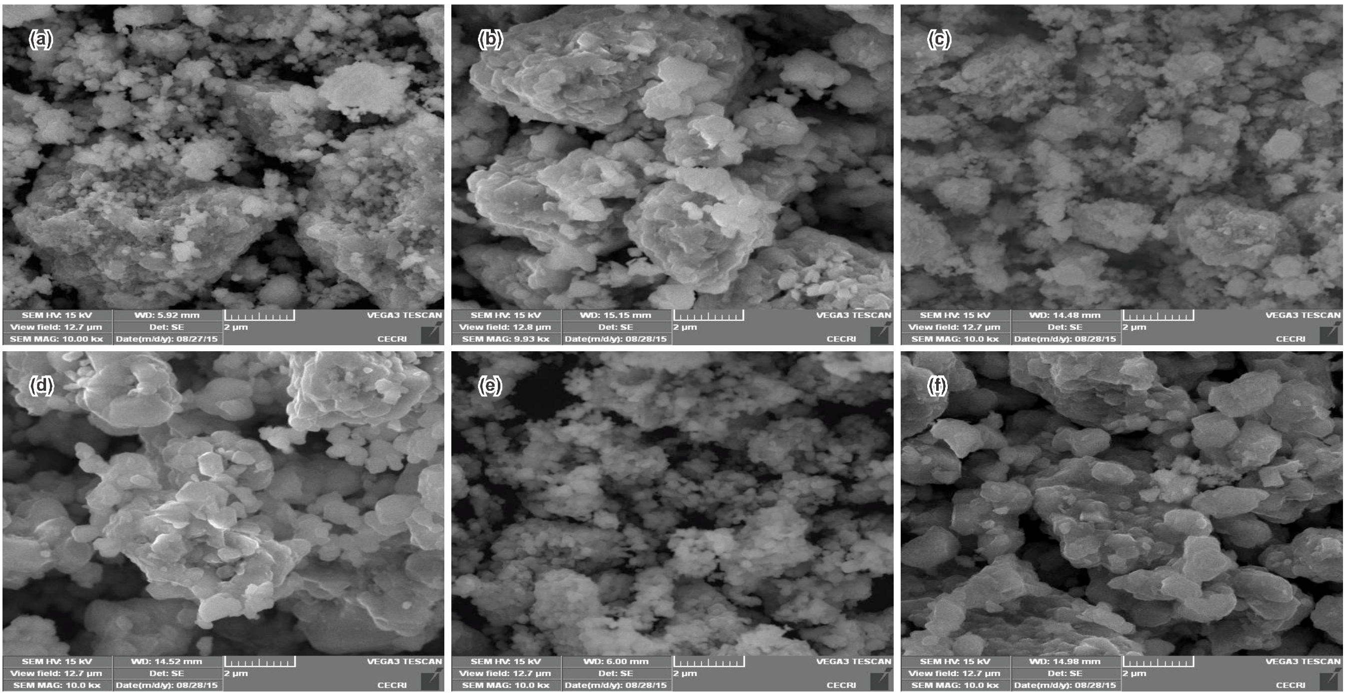

Fig. 2. SEM images of bare and Zn doped $LiNi_{0.3}Mn_{0.3}Co_{0.3}O_2$ cathode materials (a) x = 0.00 at 800 °C, (b) x = 0.00 at 1000 °C, (c) x = 0.01 at 800 °C, (d) x = 0.01 at 1000 °C, (e) x = 0.02 at 800 °C & (f) x = 0.02 at 1000 °C

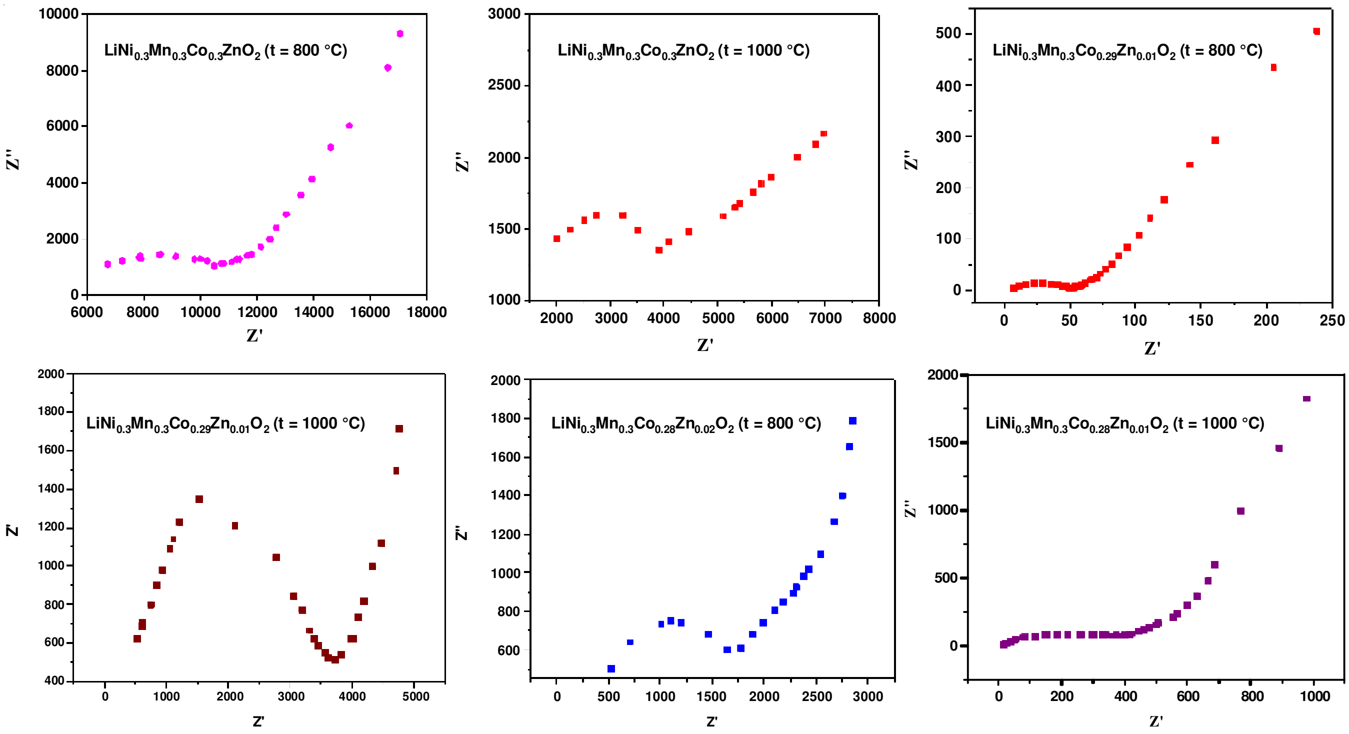

Fig. 3. Nyquist plots of the bare and Zn doped LiNi$_{0.3}$Mn$_{0.3}$Co$_{0.3}$O$_2$ cathode materials

Electrochemical impedance spectroscopy: Electrochemical impedance spectroscopy (EIS) has been used widely to evaluate the electro kinetic activity of lithium ion between cathode and anode in electrochemical cells. Fig. 3 shows the Nyquist plots of the bare and Zn doped cathode materials. After conditioning cycles, the electrodes are subjected to electrochemical impedance analysis and the spectra were recorded at the fully discharged state (*i.e.*, state-of-charge, SOC = 0) to ensure that the active material is fully saturated with lithium. The semicircle at high frequency is due to the contact impedance between the electrode material and current collector. The sloping line at low frequency can be attributed to the lithium diffusion in solid phase. Both electrodes are prepared in the same way to obtain similar contacts between particles.

The solution resistance (R_s) and charge transfer resistance (R_{ct}) values are derived from the EIS spectra of the bare and Zn doped cathode materials. The values of R_s and R_{ct} for the Zn substituted cathode material (x = 0.01) calcined at 1000 °C are very low compared to other bare and Zn substituted cathode materials. The values of R_s and R_{ct} for all the electrode materials are presented in Table-1. The data from EIS measurements show that better electrochemical performance is achieved by the zinc doping due to the more stable lattice structure and enhanced conductivity.

TABLE-1
SOLUTION RESISTANCE AND CHARGE TRANSFER RESISTANCE VALUES

Cathode materials	R_s (kΩ)	R_{ct} (kΩ)
LiNi$_{0.3}$Mn$_{0.3}$Co$_{0.3}$ Zn$_0$O$_2$ (t =800 °C)	3.5847	10.2990
LiNi$_{0.3}$Mn$_{0.3}$Co$_{0.3}$Zn$_0$O$_2$ (t =1000 °C)	0.0215	5.2084
LiNi$_{0.3}$Mn$_{0.3}$Co$_{0.3-x}$Zn$_{0.01}$O$_2$ (t = 800 °C)	5.2083	0.0466
LiNi$_{0.3}$Mn$_{0.3}$Co$_{0.29}$Zn$_{0.01}$O$_2$ (t = 1000 °C)	0.0206	2.1238
LiNi$_{0.3}$Mn$_{0.3}$Co$_{0.28}$Zn$_{0.02}$O$_2$ (t = 800 °C)	0.1249	3.4702
LiNi$_{0.3}$Mn$_{0.3}$Co$_{0.28}$Zn$_{0.02}$O$_2$ (t = 1000 °C)	0.0024	47.7670

Electrochemical performance: Fig. 4 shows the coin cells assembled with bare and Zn substituted cathodes. The discharge characteristics of bare and Zn substituted cathode materials are presented in Fig. 5. The capacity values are presented in Fig. 6. The bare and Zn-substituted cathode materials show an initial capacities [12] of 183, 180, 175, 170, 165 and 165 mAh g^{-1} for x = 0.01 (1000 °C) x = 0.02 (1000 °C) x = 0.02 (800 °C) x = 0.00 (1000 °C) x = 0.01 (800 °C) and x = 0.00 (800 °C) respectively. The Zn-substituted samples x = 0.01(1000 °C) and x = 0.02 (1000 °C) shows good capacity retention up to 30 charge–discharge cycles. The decrease in capacity with increase in Zn content is due to the decrease in electrochemically active Mn^{2+} ions.

Conclusion

In this work LiNi$_{0.3}$Mn$_{0.3}$Co$_{0.3}$O$_2$ cathode material is successfully doped with Zn *via* sol-gel process. The samples were finally calcined at 800 and 1000 °C for 10 h and the samples are characterized by X-ray diffraction, scanning

Fig. 4. Coin cells with bare and Zn substituted cathodes

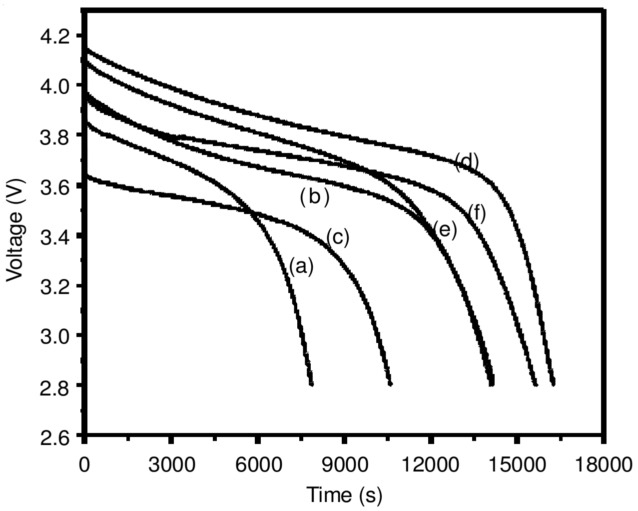

Fig. 5. Discharge curves of bare and Zn substituted cathode materials (a) x = 0.00 at 800 °C, (b) x = 0.00 at 1000 °C, (c) x = 0.01 at 800 °C, (d) x = 0.01 at 1000 °C, (e) x = 0.02 at 800 °C and (f) x = 0.02 at 1000 °C

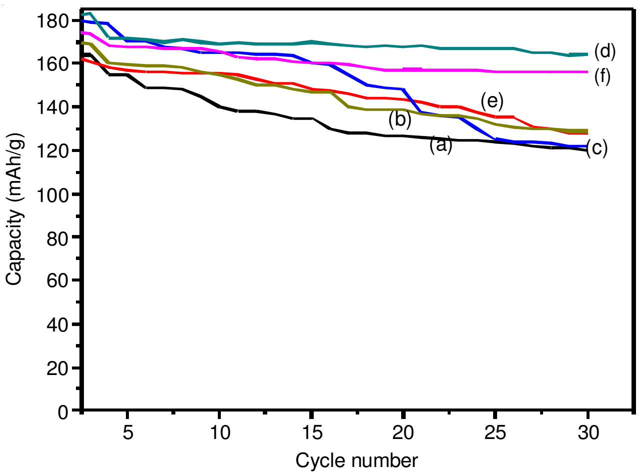

Fig. 6. Capacity curves of bare and Zn substituted cathode materials (a) x = 0.00 at 800 °C, (b) x = 0.00 at 1000 °C, (c) x = 0.01 at 800 °C, (d) x = 0.01 at 1000 °C, (e) x = 0.02 at 800 °C and (f) x = 0.02 at 1000 °C

electron microscopy, electrochemical impedance spectroscopy and galvanostatic charge/discharge. The sol-gel synthesized Li $Ni_{0.3}Mn_{0.3}Co_{0.29}Zn_{0.01}O_2$ cathode material heated at 1000 °C exhibited X-ray diffraction pattern indicating sharp and high intensity peaks due to crystallinity. The SEM images showed particles of good crystallinity. The images indicate uniform spherical morphology and particle size ranges from 200 and 250 nm for calcinations at 800 and 1000 °C, respectively. The EIS results strongly suggest that the effect of the Zn doping forms a protective layer relating to the region between the electrode surface and electrolyte and thereby prevents electrolyte decomposition. Zinc doping influences expansion of lattice volume and thereby acco-mmodates more number of lithium ions by intercalation/de-intercalation. In addition, the doping decreases the charge transfer resistance, improves the reversibility of lithium intercalation and de-intercalation and increases the diffusion of lithium ions due to the pillar effect of the Zn doped cathode materials. As a result, zinc doping is very promising for the improvement of the electrochemical performance of $LiNi_{0.3}Mn_{0.3}Co_{0.3}O_2$ cathode materials.

ACKNOWLEDGEMENTS

One of the authors, D. Deivamani acknowledges UGC-SERO, Hyderabad, India for granting FDP fellowship for carrying out this research work.

REFERENCES

1. M. Choi, G. Ham, B.-S. Jin, S.-M. Lee, Y.M. Lee, G. Wang and H.-S. Kim, *J. Alloys Comp.*, **608**, 110 (2014); https://doi.org/10.1016/j.jallcom.2014.04.068.
2. Y. Zeng, K. Qiu, Z. Yang, F. Zhou, L. Xia and Y. Bu, *Ceram. Int.*, **42**, 10433 (2016); https://doi.org/10.1016/j.ceramint.2016.03.189.
3. X. Zhang, W.J. Jiang, A. Mauger, F. Qilu, F. Gendron and C.M. Julien, *J. Power Sources*, **195**, 1292 (2010); https://doi.org/10.1016/j.jpowsour.2009.09.029.
4. H. Lee, D.J. Lee, Y.-J. Kim, J.-K. Park and H.-T. Kim, *J. Power Sources*, **284**, 103 (2015); https://doi.org/10.1016/j.jpowsour.2015.03.004.
5. Y. Chen, R. Chen, Z. Tang and L. Wang, *J. Alloys Comp.*, **476**, 539 (2009); https://doi.org/10.1016/j.jallcom.2008.09.055.
6. R. Guo, P. Shi, X. Cheng and L. Sun, *Electrochim. Acta*, **54**, 5796 (2009); https://doi.org/10.1016/j.electacta.2009.05.034.
7. P. Suresh, A.K. Shukla and N. Munichandraiah, *J. Power Sources*, **161**, 1307 (2006); https://doi.org/10.1016/j.jpowsour.2006.06.098.
8. C. Deng, S. Zhang, S.Y. Yang, B.L. Fu and L. Ma, *J. Power Sources*, **196**, 386 (2011); https://doi.org/10.1016/j.jpowsour.2010.06.064.
9. R. Santhanam and B. Rambabu, *Int. J. Electrochem. Sci.*, **4**, 1770 (2009).
10. D. Deivamani and P. Perumal, *Int. J. Chem. Sci.*, **14**, 496 (2016).
11. W. Ahn, S.N. Lim, K.-N. Jung, S.-H. Yeon, K.B. Kim, H.S. Song, K.-H. Shin, *J. Alloys Comp.*, **609**, 143 (2014); https://doi.org/10.1016/j.jallcom.2014.03.123.
12. L. Zhang, K. Jin, L. Wang, Y. Zhang, X. Li and Y. Song, *J. Alloys Comp.*, **638**, 298 (2015); https://doi.org/10.1016/j.jallcom.2015.03.100.